PAPER

Check for updates

Design, synthesis and biological evaluation of 2,3-dihydroimidazo[1,2-c]quinazoline derivatives as novel phosphatidylinositol 3-kinase and histone deacetylase dual inhibitors†

Yichao Wu,[a] Weichen Dai,[ab] Xin Chen,[ac] Aixin Geng,[a] Yadong Chen,[d] Tao Lu*[ad] and Yong Zhu 📵 *[a]

Histone deacetylase (HDAC) inhibitors are known to induce multiple epigenetic modifications affecting signaling networks and act synergistically with phosphatidylinositol 3-kinase (PI3K) inhibitors for the treatment of cancer. Herein we present a novel design approach for cancer drug development by incorporating HDAC inhibitory functionality into a PI3K inhibitor pharmacophore to construct dual-acting inhibitors. The designed compounds were synthesized and showed inhibitory activities against PI3K and HDAC. The representative dual PI3K/HDAC inhibitors, compounds **12a–j**, showed potent antiproliferative activities against K562 and Hut78 in cellular assays. This work may lay the foundation for developing novel dual PI3K/HDAC inhibitors as potential anticancer therapeutics.

Introduction

The phosphoinositide 3-kinase (PI3K) family of lipid kinases generate 3′-phosphoinositides that activate a variety of cellular targets important for cell proliferation, survival, differentiation, and migration.[1,2] Collectively, PI3Ks act as intermediate signaling molecules and activate the serine–threonine kinase AKT and other downstream effectors.[3] Based on their primary structure and mechanism of action, PI3Ks are divided into three major classes: class I, II, and III.[4–6] Class I PI3K is composed of a catalytic subunit, p110, and a regulatory subunit, p85 or p101. The catalytic subunit consists of four isoforms: p110α, β, γ, δ.[7] In many human cancers, the *PIK3CA* gene that encodes p110α is also frequently mutated. Thus class I PI3Ks, particularly p110α, are potential therapeutic targets for cancers.[8,9] Over the past decade, researchers have made significant progress in developing pan-PI3K or isoform-specific PI3K inhibitors, such as pictilisib, GSK1059615, PI-103 and copanlisib, which have shown promising activity against various types of cancers and most are currently under clinical investigation (Fig. 1).[10] Unfortunately, numerous studies reported that the efficacy of PI3K inhibitors is limited by concurrent activation of other survival- and growth-related pathways.[11,12]

In addition to genetic mutations, epigenetic changes, such as dysregulation of histone deacetylases (HDAC), contribute to cancer cell initiation and growth, by altering the cell phenotype and gene expression and by disturbing homeostasis.[13] Thus, HDAC inhibitors are emerging drugs for cancer therapeutics.[14] Extensive efforts have resulted in the identification of many potent HDAC inhibitors, including vorinostat (SAHA), belinostat (PXD-101), and panobinostat (LBH-589), which have been approved by the FDA, respectively, to treat cutaneous T-cell lymphoma (CTCL), peripheral T-cell lymphoma (PTCL), and multiple myeloma (MM) (Fig. 2). Several small molecule HDAC inhibitors have entered clinical trials for the treatment of a variety of haematological and solid tumors.[15]

Recently, it has been reported that the combination of an HDAC inhibitor and a kinase inhibitor, such as epidermal growth factor receptor (EGFR) tyrosine kinase inhibitor or PI3K inhibitor, can overcome kinase inhibitor resistance and induce apoptosis in human solid cancers in a synergistic manner.[16–18] Therefore, development of inhibitors targeting both HDAC and PI3K would be advantageous as anticancer drug candidates. Indeed, a dual inhibitor of HDAC and PI3K, CUDC-907, is currently under evaluation in phase I clinical trials in patients with lymphoma or multiple myeloma, and in patients with advanced solid tumors.[19,20] Another HDAC inhibitor, FK228, has been also demonstrated to directly inhibit PI3K activity and potently induce apoptosis through HDAC/PI3K dual inhibition

[a]Department of Organic Chemistry, School of Science, China Pharmaceutical University, 639 Longmian Avenue, Nanjing 211198, China. E-mail: lutao@cpu.edu.cn; zhuyong@cpu.edu.cn; Fax: +86-25-86185179; +86-25-86185182

[b]Department of Medicinal Chemistry, School of Pharmacy, Nanjing University of Chinese Medicine, Hanlin College, 6 Xueyuan Road, Taizhou 225300, China

[c]Shanxi Key Laboratory of Natural Products & Chemical Biology, College of Science, Northwest A&F University, Yangling 712100, China

[d]Laboratory of Molecular Design and Drug Discovery, School of Science, China Pharmaceutical University, 639 Longmian Avenue, Nanjing 211198, China

† Electronic supplementary information (ESI) available: Details of experimental procedure, spectral data of all novel compounds. See DOI: 10.1039/c7ra08835c
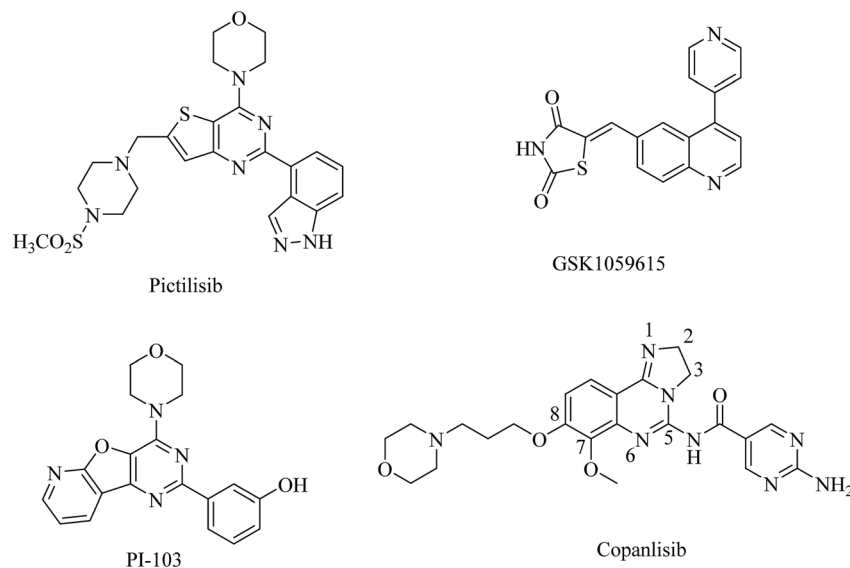
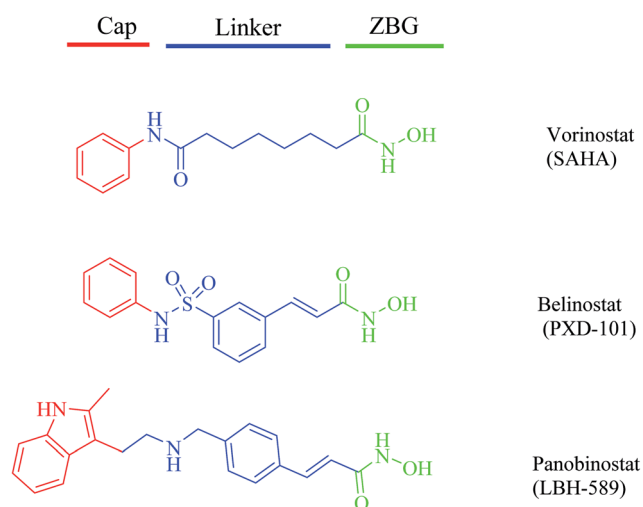**Fig. 1** Representative structures of PI3K inhibitors.

Fig. 2 Representative structures of HDAC inhibitors.

(Fig. 3).[21] The evidence has suggested that simultaneous PI3K and HDAC inhibition could be a promising approach in cancer therapy.

In this report, we designed and synthesized a novel series of dual-acting PI3K and HDAC inhibitors by incorporating HDAC inhibitory functionality into a PI3K inhibitor pharmacophore.[22] The rationale for the dual-inhibitor design originated from our deep insights into previously reported X-ray crystal structure of copanlisib bound to PI3K (Fig. 4A) and vorinostat bound to a HDAC homolog (Fig. 4B).[23,24] The imidazoline N1 nitrogen of copanlisib forms a critical hydrogen bond to V882 in the adenine pocket so as to possess strong hinge interactions. The C5 aminopyrimidine group fills the affinity pocket, forming hydrogen bonds with D836 and D841 through the amino group, and with K833 through a pyrimidine nitrogen. In addition, D964 appears to contribute a π-stacking interaction. Finally, the morpholine group of copanlisib lies over W812, and points to solvent. The long alkyl chain of vorinostat is located in a long narrow tubular channel. Hydroxamate forms three hydrogen bonds with Y297, H131 and H132, respectively. The capping phenyl group binds to the hydrophobic part on the protein surface. It is well established that the pharmacophore of HDAC inhibitors (Fig. 2) consists of a capping group, an appropriate linker and a zinc-binding group (ZBG). Generally, ZBG plays a significant role in the binding efficiency between HDAC
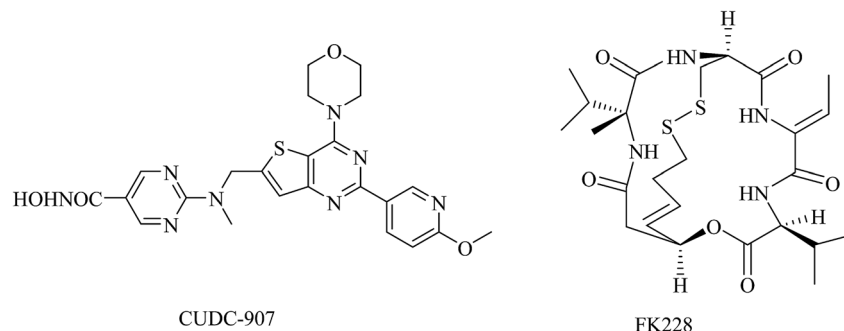

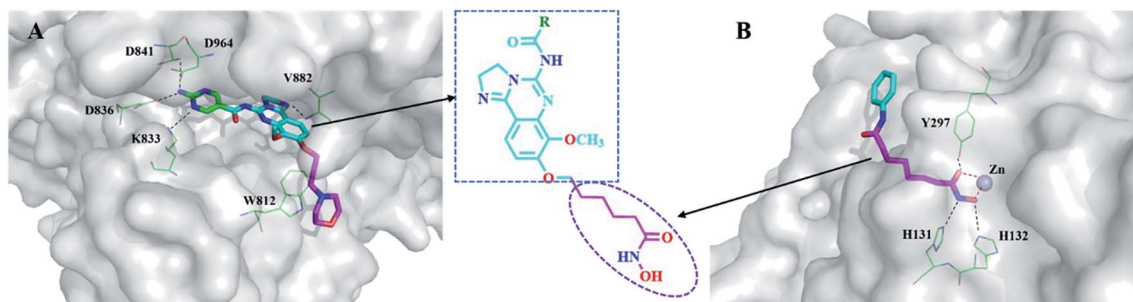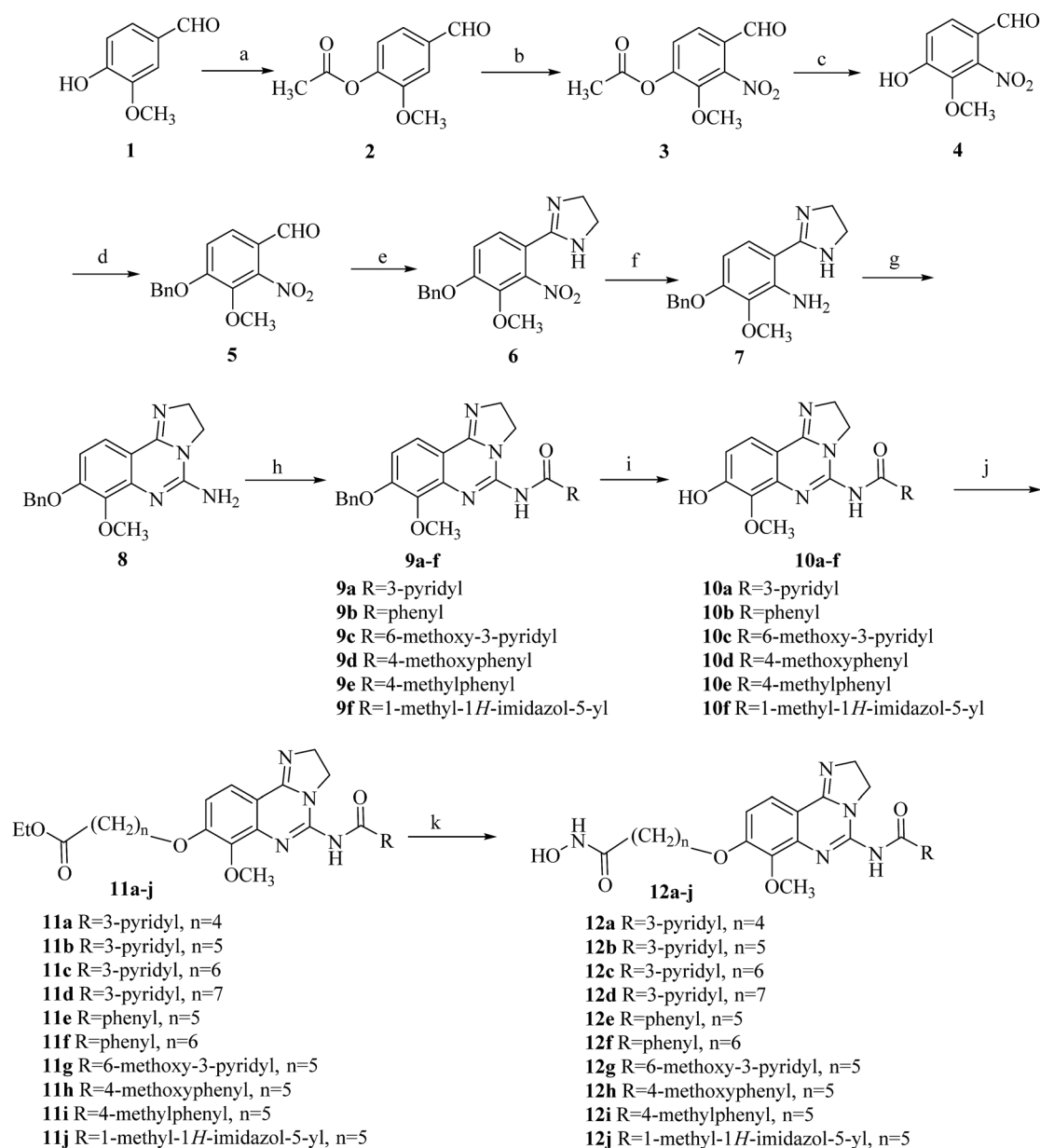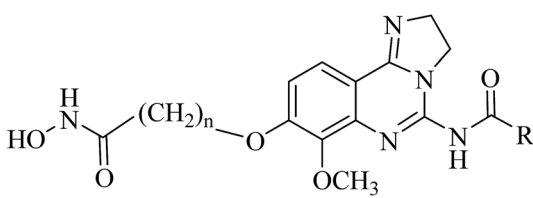**Fig. 3** Representative structures of PI3K/HDAC dual inhibitors.
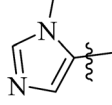
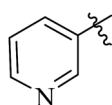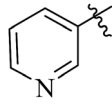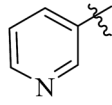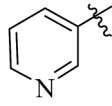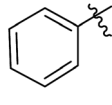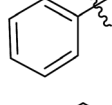**Fig. 4** Design of dual inhibitors of PI3K/HDAC. (A) X-ray crystal structures of copanlisib bound to PI3K (PDB entry: 5G2N), (B) vorinostat docked to an HDAC1 homolog (PDB entry: 1C3S). The proteins are shown as white surface or cartoon. Copanlisib and vorinostat are shown in sticks. The hydrogen bonds were denoted by black dash lines. Figures were prepared using PyMOL.

9a R=3-pyridyl
9b R=phenyl
9c R=6-methoxy-3-pyridyl
9d R=4-methoxyphenyl
9e R=4-methylphenyl
9f R=1-methyl-1H-imidazol-5-yl

10a R=3-pyridyl
10b R=phenyl
10c R=6-methoxy-3-pyridyl
10d R=4-methoxyphenyl
10e R=4-methylphenyl
10f R=1-methyl-1H-imidazol-5-yl

11a R=3-pyridyl, n=4
11b R=3-pyridyl, n=5
11c R=3-pyridyl, n=6
11d R=3-pyridyl, n=7
11e R=phenyl, n=5
11f R=phenyl, n=6
11g R=6-methoxy-3-pyridyl, n=5
11h R=4-methoxyphenyl, n=5
11i R=4-methylphenyl, n=5
11j R=1-methyl-1H-imidazol-5-yl, n=5

12a R=3-pyridyl, n=4
12b R=3-pyridyl, n=5
12c R=3-pyridyl, n=6
12d R=3-pyridyl, n=7
12e R=phenyl, n=5
12f R=phenyl, n=6
12g R=6-methoxy-3-pyridyl, n=5
12h R=4-methoxyphenyl, n=5
12i R=4-methylphenyl, n=5
12j R=1-methyl-1H-imidazol-5-yl, n=5

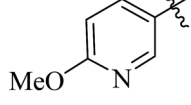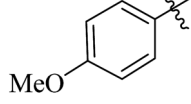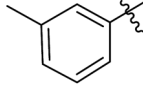**Scheme 1** Reagent and conditions: (a) $(CH_3CO)_2O$, Et_3N, DMAP, rt, 3 h; (b) fuming HNO_3, <5 °C, 2 h; (c) KOH, H_2O, 100 °C, 15 min; (d) BnBr, K_2CO_3, DMF, rt, 4 h; (e) $NH_2CH_2CH_2NH_2$, I_2, K_2CO_3, $(CH_3)_3COH$, 85 °C, 4 h; (f) Fe, AcOH, H_2O, rt, 24 h; (g) BrCN, TEA, CH_2Cl_2, 0 °C to rt, 4 h; (h) RCOCl, Et_3N, CH_2Cl_2, 0 °C to rt; (i) TFA, 60 °C, 5 h; (j) $Br(CH_2)_nCO_2Et$, Cs_2CO_3, DMF, 80 °C, 2 h; (k) $NH_2OH \cdot HCl$, KOH, MeOH, rt.

Table 1 IC_{50} values of compounds **12a–12j** against HDAC1 and $PI3K\alpha^a$

Compd.	R	n	IC_{50} of HDAC1^b (nM)	IC_{50} of PI3Kα^b (nM)
12a		4	4430	2.79
12b		5	107	1.35
12c		6	86	1.72
12d		7	339	2.08
12e		5	50	2.98
12f		6	91	3.33
12g		5	82	1.92
12h		5	172	4.65
12i		5	162	4.31
12j		5	240	10.95
Vorinostat			52	ND
Copanlisib			ND	1.42

^{a} ND: not determined. ^{b} Values were the average of three experiments, SD < 10%.

inhibitors and enzyme. Hydroxamate is one of the most potent zinc ion chelating group among all types of ZBGs. Given the known binding modes of the PI3K inhibitor copanlisib and HDAC inhibitor vorinostat, it was envisaged that amalgamation of these pharmacophores would be a viable strategy to single molecules retaining both activities. We postulated that introduction of the linker and ZBG of vorinostat to the position C8 of copanlisib would be compatible with HDAC inhibition since that the channel pointing toward solvent of PI3K and the tubular channel of HDAC share considerable similarities

(Fig. 4). The linker and ZBG of vorinostat may direct into the solvent to make it well occupied which may increase the affinity to PI3K. In the meantime, 2,3-dihydroimidazo[1,2-*c*]-quinazoline moiety of copanlisib may bind to the HDAC surface as the surface recognition capping group. The fused molecules were expected to retain the essential interactions with both proteins to exert desired biological functions.

Results and discussion

Chemistry

The synthetic route of **12a–12j** were outlined in Scheme 1.[23,25] Vanillin was protected with acetate group, then was nitrated with fuming nitric acid to readily afford aldehyde **3**. The acetate group of compound **3** was removed to provide phenol **4**. Conversion into benzyl ether **5** followed ethanediamine/iodine oxidation gave the ring of 4,5-dihydro-1*H*-imidazole **6**. Reduction provided aniline **7**, and treatment with cyanogen bromide to give tricyclic amine **8**, which was acylated using a variety of different acid chlorides to provide amide **9a–9f**. Treatment of amide **9a–9f** with trifluoroacetic acid afforded deprotected phenol **10a–10f**, which could then be alkylated at C8 giving access to the aryl ethers **11a–11j**. Finally, the ethyl ester groups of compounds **11a–11j** were treated with freshly prepared hydroxylamine in methanol to produce target compounds **12a–12j**.

Biological assays

***In vitro* HDAC and PI3K inhibition.** To study the biological activity, compounds **12a–12j** were evaluated against HDAC1 enzyme assay with vorinostat as a positive control and PI3Kα activity assay with copanlisib as a positive control using the fluorimetric activity assay.[22,26] As shown in Table 1, most compounds exhibited moderate to good inhibitory activity against both PI3Kα and HDAC1. The length of the hydroxamic acid side chains of this series have marginal effects on HDAC1 inhibition (**12b** > **12c** > **12d** > **12a**) and the optimal carbon chain length is five or six carbon atoms, such as **12b** (IC_{50} = 107 nM) and **12c** (IC_{50} = 86 nM), **12e** (IC_{50} = 50 nM) and **12f** (IC_{50} = 91 nM). Diversity in the length of side chains are tolerable to PI3K inhibition due to the long channel pointing to solvent of protein. These results illustrated that the linker between the hydroxamic acid side chain and the 2,3-dihydroimidazo[1,2-*c*] quinazoline skeleton has relatively significant effect on HDAC1 inhibition, but has little effect on PI3Kα protency.

Variation of the aromatic C5 amides moiety had significant effect on p110α potency (Table 1). Nicotinamide and substituted nicotinamide moiety exhibited almost the similar inhibitory activities against PI3K to copanlisib. Benzyl or substituted benzyl amides, such as **12e** (IC_{50} = 2.89 nM) and **12f** (IC_{50} = 3.33 nM), were slightly less active than compounds **12b** (IC_{50} = 1.35 nM) and **12c** (IC_{50} = 1.72 nM) with pyridine moiety. The same trends were observed in compounds **12g** and **12h**. This decreased activity may be due to the inability of these amides to act as hydrogen-bond acceptors. In addition, the five-membered heterocyclic amide **12j** were significantly less active than six-membered aryl amides, such as **12b** and **12e**. This result may

suggest that six-membered aromatic cycles are preferred to fit in the affinity pocket.

In order to further ascertain the pan-inhibition of HDAC enzymes and class I PI3K kinases, three representative compounds **12b**, **12c** and **12e** with better HDAC1 and PI3Kα inhibition were selected and evaluated against recombinant human HDAC1, HDAC6, HDAC8 enzymes and PI3Kα, β, γ, δ, using vorinostat and copanlisib as the positive control compound. As shown on Table 2, it is noteworthy that this set of structures show promising pan-inhibition for HDACs and PI3Ks.

***In vitro* cell growth inhibition.** To test the anticancer activities of the synthesized compounds, we evaluated antiproliferative activities of representative compounds **12b**, **12c**, **12e**, **12h** and **12i** against human colon cancer cell line (HCT116), human leukemia cell line (K562), and cutaneous T lymphocyte (Hut78) by applying the MTT colorimetric assay. The IC_{50} values were summarized on Table 3. According to the inhibition data, all tested compounds showed obvious antiproliferative activities. Consistent with this observation of HDAC and PI3K inhibition, we found that **12b**, **12c** and **12e** potently inhibits the growth of those cancer cells derived from both hematologic and solid tumors. Especially, compound **12e** exhibited the better anti-proliferative activity in K562 and Hut78 cell lines than vorinostat and copanlisib.

Molecular docking studies

For further understanding of the interaction between these inhibitors and proteins (HDAC1 and PI3K) and guiding the

Table 2 Inhibition of HDAC and PI3K isoforms by compound **12b**, **12c** and **12e**[a]

Compd.	IC_{50}^{b} (nM)						
	HDAC1	HDAC6	HDAC8	PI3Kα	PI3Kβ	PI3Kγ	PI3Kδ
12b	107	97	327	1.35	10.2	19.3	1.97
12c	86	162	412	1.72	9.6	15.8	2.02
12e	50	62	153	2.98	14.2	29.5	4.52
Vorinostat	52	43	187	ND	ND	ND	ND
Copanlisib	ND	ND	ND	1.42	9.12	16.3	1.72

[a] ND: not determined. [b] Values were the average of three experiments, SD < 10%.

Table 3 Antiproliferative activities of compounds **12b**, **12c**, **12e**, **12h** and **12i**

Compd.	IC_{50}^{a} (μM)		
	HCT116	K562	Hut78
12b	0.52	0.32	0.17
12c	0.41	0.48	0.21
12e	0.33	0.095	0.062
12h	0.89	0.77	0.51
12i	0.64	0.53	0.15
Vorinostat	1.17	0.21	0.092
Copanlisib	0.26	0.73	0.12

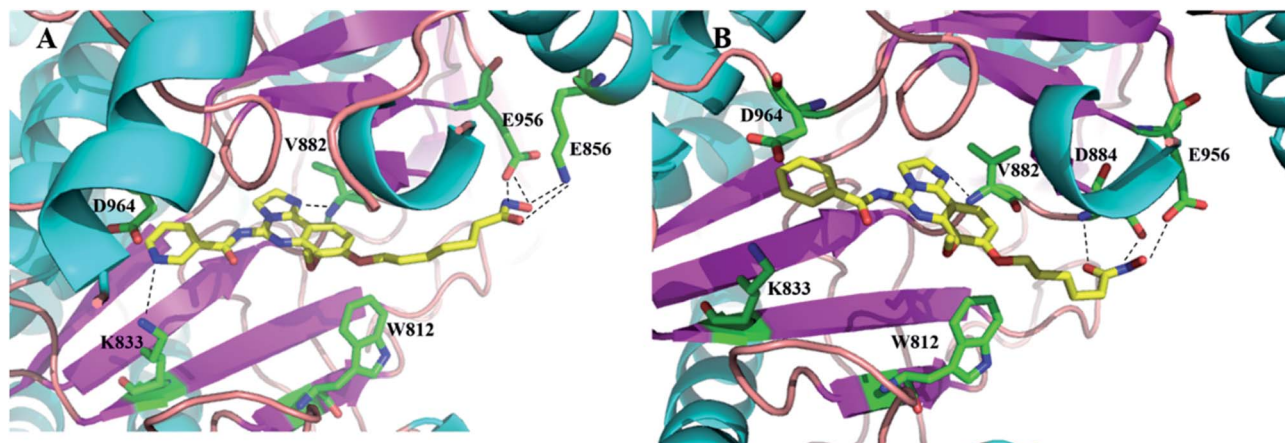[a] Values were the average of two experiments, SD < 10%.

Fig. 5   The docking model of compounds **12c** (A) and **12e** (B) bound to PI3K (PDB entry 5G2N). **12c** and **12e** are represented by tube and colored by atom type (C, yellow; N, blue; O, red). The hydrogen bonds are denoted by black dash lines. The protein is shown as ribbons. The key amino acids forming the pocket are represented by tube with carbon atoms colored in green, oxygen atoms in red and nitrogen atoms in blue. Figures were prepared using PyMOL.

structure–activity relationships, a molecular docking was performed using the C-DOCKER program within Discovery Studio 2.5 software package. We docked the representative compound **12c** and **12e**, the most potent compound of this series, in the active site of PI3K (PDB code: 5G2N) (Fig. 5) and HDAC homolog (PDB code: 1C3R) (Fig. 6), revealing excellent shape complementarity between ligand and the binding pocket. As shown in Fig. 5A and B, compound **12c** and **12e** have the binding mode similar to that of copanlisib as we expected. 2,3-Dihydroimidazo[1,2-*c*]quinazoline moiety occupied the ATP binding pocket. And the imidazoline N1 nitrogen forms a critical hydrogen bond to Val882 in the protein hinge region. The morpholine group lies over Trp812, apparently adding a hydrophilic shield to the hydrophobic heterocycle. The C5 aryl amide group appears to contribute a π-stacking interaction on Asp964. The C5 pyrimidine group of compound **12c** can form a hydrogen bond with

Lys833 through a pyrimidine nitrogen, but the compound **12e** loses the hydrogen. This could be the reason that the compound **12e** has a slightly lower activity against PI3K than compound **12b** and **12c**. In addition, the long alkyl chain at C8 of compound **12c** and **12e** just fits into the channel pointing toward solvent, and hydroxamate forms three or four hydrogen bonds with the residues located at the solvent. The docking mode of **12c** and **12e** in complex with HDAC reveals that this compound binds in the HDAC pocket in a similar manner and forms the same interactions as vorinostat (Fig. 6A and B). The hydroxamic acid group anchors **12c** and **12e** into the active site by chelating the essential catalytic zinc ion. Hydroxamate forms three hydrogen bonds with Y297, H131 and H132, respectively. The long alkyl chain of **12c** and **12e** exits the reaction centre along the long narrow tubular channel. 2,3-Dihydroimidazo[1,2-*c*]quinazoline moiety was placed in an open environment of the
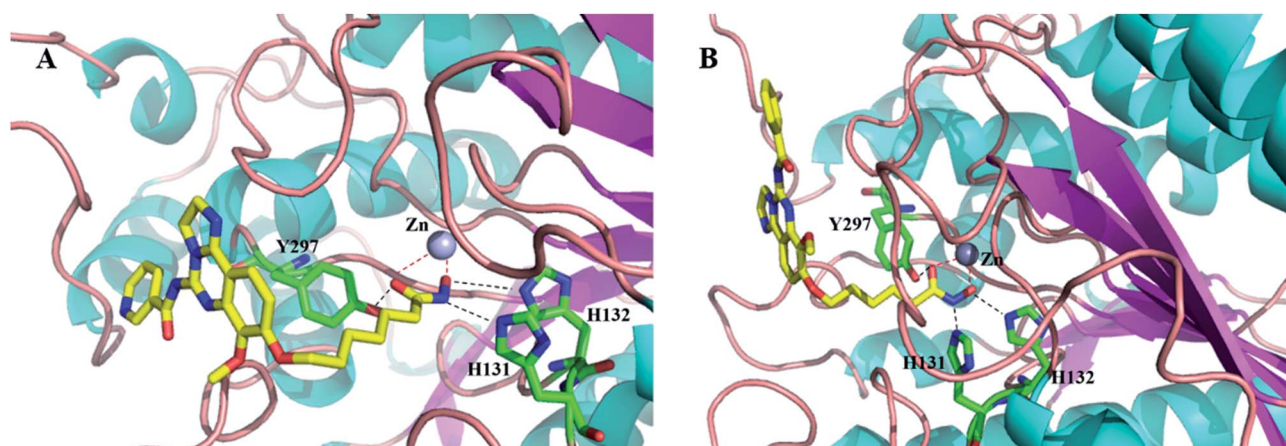

Fig. 6   The docking model of compounds **12c** (A) and **12e** (B) bound to HDAC1 (PDB entry 1C3S). **12c** and **12e** are represented by tube and colored by atom type (C, yellow; N, blue; O, red). The hydrogen bonds are denoted by black dash lines and chelation is shown by red dash lines. The protein is shown as ribbons. The key amino acids forming the pocket are represented by tube with carbon atoms colored in green, oxygen atoms in red and nitrogen atoms in blue and zinc in grey. Figures were prepared using PyMOL.

protein surface and projects outward into the solvent, corresponding to the fact that the SARs of the HDACs inhibitors do not strongly depend on variations in this region.

Conclusions

In summary, using structure-based design approach, we have successfully designed and synthesized a novel series of 2,3-dihydroimidazo [1,2-c]quinazoline with a hydroxamate group essential for chelation with the zinc ion in the active site of HDAC as novel PI3K/HDAC dual inhibitors. As expected, most of compounds exhibited distinct high to moderate inhibitory activities against both HDAC1 and PI3Kα. Moreover, the selectivity assay of compounds **12b**, **12c** and **12e** shows that they are excellent pan inhibitors for HDACs and PI3Ks. In addition, compound **12e** showed the most potent inhibitory activity against K562 and Hut78. By combining two distinct pharmacophores into one molecule, we have demonstrated the example of PI3K/HDAC dual inhibitors as a promising approach to search for efficient anticancer multi-target agents.

Conflicts of interest

There are no conflicts to declare.

Acknowledgements

Notes and references

1 L. C. Cantley, *Science*, 2002, **296**, 1655–1657.
2 M. Osaki, M. Oshimura and H. Ito, *Apoptosis*, 2004, **9**, 667–676.
3 P. Liu, H. Cheng, T. M. Roberts and J. J. Zhao, *Nat. Rev. Drug Discovery*, 2009, **8**, 627–644.
4 M. Hayakawa, K. Kawaguchi, H. Kaizawa, T. Koizumi, T. Ohishi, M. Yamano, M. Okada, M. Ohta, S. Tsukamoto, F. I. Raynaud, P. Parker, P. Workman and M. D. Waterfield, *Bioorg. Med. Chem.*, 2007, **15**, 5837–5844.
5 M. A. Lawlor and D. R. Alessi, *J. Cell Sci.*, 2001, **114**, 2903–2910.
6 V. Kumar and M. I. Siddiqi, *RSC Adv.*, 2016, **6**, 112455–112467.
7 B. T. Hennessy, D. L. Smith, P. T. Ram, Y. Lu and G. B. Mills, *Nat. Rev. Drug Discovery*, 2005, **4**, 988–1004.
8 Y. Samuels, Z. Wang, A. Bardelli, N. Silliman, J. Ptak, S. Szabo, H. Yan, A. Gazdar, S. M. Powell, G. J. Riggins, J. K. Willson, S. Markowitz, K. W. Kinzler, B. Vogelstein and V. E. Velculescu, *Science*, 2004, **304**, 554.
9 M. Martini, E. Ciraolo, F. Gulluni and E. Hirsch, *Front. Oncol.*, 2013, **3**, 108.
10 C. Garcia-Echeverria and W. R. Sellers, *Oncogene*, 2008, **27**, 5511–5526.
11 F. I. Raynaud, S. Eccles, P. A. Clarke, A. Hayes, B. Nutley, S. Alix, A. Henley, F. Di-Stefano, Z. Ahmad, S. Guillard, L. M. Bjerke, L. Kelland, M. Valenti, L. Patterson, S. Gowan, A. de Haven Brandon, M. Hayakawa, H. Kaizawa, T. Koizumi, T. Ohishi, S. Patel, N. Saghir, P. Parker, M. Waterfield and P. Workman, *Cancer Res.*, 2007, **67**, 5840–5850.
12 M. L. Sos, S. Fischer, R. Ullrich, M. Peifer, J. M. Heuckmann, M. Koker, S. Heynck, I. Stuckrath, J. Weiss, F. Fischer, K. Michel, A. Goel, L. Regales, K. A. Politi, S. Perera, M. Getlik, L. C. Heukamp, S. Ansen, T. Zander, R. Beroukhim, H. Kashkar, K. M. Shokat, W. R. Sellers, D. Rauh, C. Orr, K. P. Hoeflich, L. Friedman, K. K. Wong, W. Pao and R. K. Thomas, *Proc. Natl. Acad. Sci. U. S. A.*, 2009, **106**, 18351–18356.
13 A. C. West and R. W. Johnstone, *J. Clin. Invest.*, 2014, **124**, 30–39.
14 A. A. Lane and B. A. Chabner, *J. Clin. Oncol.*, 2009, **27**, 5459–5468.
15 J. Tan, S. Cang, Y. Ma, R. L. Petrillo and D. Liu, *J. Hematol. Oncol.*, 2010, **3**, 5.
16 T. Nakagawa, S. Takeuchi, T. Yamada, H. Ebi, T. Sano, S. Nanjo, D. Ishikawa, M. Sato, Y. Hasegawa, Y. Sekido and S. Yano, *Cancer Res.*, 2013, **73**, 2428–2434.
17 T. Yoshioka, S. Yogosawa, T. Yamada, J. Kitawaki and T. Sakai, *Gynecol. Oncol.*, 2013, **129**, 425–432.
18 W. P. Zhang, X. W. Zheng, T. Meng, H. S. You, Y. L. Dong, J. F. Xing and S. Y. Chen, *RSC Adv.*, 2016, **6**, 48072–48082.
19 C. P. Wu, Y. J. Hsieh, S. H. Hsiao, C. Y. Su, Y. Q. Li, Y. H. Huang, C. W. Huang, C. H. Hsieh, J. S. Yu and Y. S. Wu, *Mol. Pharm.*, 2016, **13**, 784–794.
20 S. Kotian, L. Zhang, M. Boufraqech, K. Gaskins, S. K. Gara, M. M. Quezado, N. Nilubol and E. Kebebew, *Clin. Cancer Res.*, 2017, **23**, 5044–5054.
21 K. Saijo, J. Imamura, K. Narita, A. Oda, H. Shimodaira, T. Katoh and C. Ishioka, *Cancer Sci.*, 2015, **106**, 208–215.
22 X. Chen, S. Zhao, Y. C. Wu, Y. D. Chen, T. Lu and Y. Zhu, *RSC Adv.*, 2016, **6**, 103178–103184.
23 W. J. Scott, M. F. Hentemann, R. B. Rowley, C. O. Bull, S. Jenkins, A. M. Bullion, J. Johnson, A. Redman, A. H. Robbins, W. Esler, R. P. Fracasso, T. Garrison, M. Hamilton, M. Michels, J. E. Wood, D. P. Wilkie, H. Xiao, J. Levy, E. Stasik, N. Liu, M. Schaefer, M. Brands and J. Lefranc, *ChemMedChem*, 2016, **11**, 1517–1530.
24 M. S. Finnin, J. R. Donigian, A. Cohen, V. M. Richon, R. A. Rifkind, P. A. Marks, R. Breslow and N. P. Pavletich, *Nature*, 1999, **401**, 188–193.
25 Y. Zhu, X. Chen, Z. Wu, Y. Zheng, Y. Chen, W. Tang and T. Lu, *Arch. Pharmacal Res.*, 2012, **35**, 1723–1732.
26 R. R. Yadav, S. K. Guru, P. Joshi, G. Mahajan, M. J. Mintoo, V. Kumar, S. S. Bharate, D. M. Mondhe, R. A. Vishwakarma, S. Bhushan and S. B. Bharate, *Eur. J. Med. Chem.*, 2016, **122**, 731–743.